Modeling of One-Dimensional Atoms and Diatomic Molecules through Density Functional Theory

An Honors Thesis (HONR 499)

by

Kyle Jones

Thesis Advisor

Dr. Antonio Cancio

Ball State University

Muncie, Indiana

May, 2019

Expected Date of Graduation

May, 2019

Abstract

We have developed a code to solve the Schrodinger equation of one-dimensional systems of electrons numerically in a plane wave basis. We have tested the accuracy of the code by performing convergence tests versus cell size and plane wave number, for the square-well and the Poschl-Teller well. We use this to calculate numerically accurate electron and kinetic energy densities and compare to simple density functional models for these quantities. We plan to use this code to investigate the results when two potential wells are pulled apart. Density functional theory (the use of only the density to calculate energies) is known to fail in three dimensions as electric bonds are broken and we expect this to be a problem in one dimension as well. Our one-dimensional code will allow for quick testing of new models and theories to see if they are viable avenues for better describing electronic bonding.

Acknowledgements

Firstly, I need to thank Dr. Cancio for the continual guidance through the process of completing this thesis. Secondly, I would like to thank my parents for their continual suupport throughout the years. Lastly, I would like to thank the Ball State Department of Physics and Astronomy and the Ball State Honors College for giving me these great opportunities.

Contents

List of Figures

Process Analysis Statement

For my honors thesis, I wished to undertake a project that utilized the skills that I had developed in both my major in physics and my minors in computer science and mathematics. The professor that I was already undertaking research with, Dr. Cancio, suggested this topic, and this sort of computational physics research seemed like an ideal way to fuse these topics. I worked on computer code to model the electron and kinetic energy densities of this system, first adapting the code in a book from C++ into Python. After making sure that the code still did what the book said it should, I altered the code to use different units and to give us the eigenvalues instead of forcing us to estimate the eigenvalues graphically like the original code did, which is much less precise. We then used the orbitals that we had calculated to calculate the particle density and kinetic energy density. This is when we found that the square-well potentials that we had been using were producing poor results due to their lack of differentiability, so we replaced them with Poschl-Teller wells, which by their nature forced us to alter our code so that the cells that we were working with were centered at 0 instead of L/2. Around this time, it became clear that my code was becoming unwiedly and difficult to work with, so I had to do a process known in computer science as refactoring, which involves breaking the code into smaller, more workable components, testing those smaller components to make sure that they work, renaming components for greater clarity, and getting rid of redundant or unneeded components. We then implemented the calculations of the non-Kohn-Sham approximations described in the rest of the thesis. Since it was taking inordinate amounts of time to make the simplest changes to plots since I would have to run the whole code to even just fix minor spelling mistakes, I separated the plotting and

calculating parts of the code by putting the results of the calculations into readable files that could be read and plotted by a seperate program, which cut down on the amount of time that I had to sit around waiting for the code to finish running. My final major alteration to the code was creating a new potential to simulate diatomic molecules, which I creatively made by just making two Poschl-Teller Wells offset by an interatomic distance variable (why make new code when I can slightly alter and repurpose existing code). For anybody attempting to read this that lacks a math, physics, or chemistry background, I would reccomend skipping most of the equations in the theory chapter while focusing on the descriptions of what the different approximations tell us. When looking at the kinetic energy approximation graphs, know that our goal is to get the approximations as close as possible to the Kohn-Sham (the black line). An approximation that is close to the black line does a good job describing the kinetic energy density of that specific system. The details are very technical and complicated, but the basic idea of what we are doing (testing methods of approximating the kinetic energy densities of atomic and molecular systems in one dimension) is (hopefully) not that hard to grasp, if the reader keeps an eye on the big picture. Working on this project, I learned how easy it is to overestimate your own abilities while doing a large project like this. I also found out how frustrating but ultimately rewarding computational physics research can be, as I would stare at code for hours trying to figure out why it was not working like I wanted it to. I learned much more about how Density Functional Theory actually operates, and I got a head start on how computational physics research works for when I go to graduate school. I also learned how to use LaTeX, software that is often used to write professional math and physics papers, which I used to write the very paper that you are reading right now. While I am about to graduate, I hope that others will pick up my code and continue this work after I leave.

Chapter 1

Introduction

Density Functional Theory (DFT), while technically existing beforehand with theories such as Thomas-Fermi (TF) theory laying the groundwork, first came into prominence as a theory when Hohenberg and Kohn formulated the foundational theorems for DFT in 1964 [1]. Hohenberg and Kohn established that the ground state properties of a system are completely determined by the electron density and that there is a correspondance between external potentials and the density [2, 1]. The energy of the electrons can be split into a term that depends only on the electron density and a term that represents the interaction energy between electrons and the atomic nuclei of a given system [1]. The first term is just the kinetic energy of the electrons and the energy of electron-electron interactions and doesn't involve the nuclei [1]. In order to find the energy of electrons in atom, a way to formulate the term dependent on the electron density is required [1]. The initial way to attempt this is the already mentioned TF theory [3, 4, 1], but this was a drastic simplification and was only accurate to within 10% of the correct energy [1]. Kohn and Sham proposed a fix by calculating the energy of the equivalent noninteracting system and including the effect of electron-electron interactions in an approximate way [2, 1]. This method is very accurate, but as it, unlike TF theory, requires the use of orbitals, it may in some cases be time consuming to calculate, albeit still an improvement over previous methods [1]. Several methods of approximating the electron-electron interaction energy emerged. The first was developed

by Kohn and Sham and is called the Local Density Approximation (LDA). LDA works by assuming that the system is a uniform electron gas and only depends on the electron density at each point. The General Gradient Approximation (GGA), which uses the electron density and its gradient at every point, was developed as an improvement over LDA [1, 5]. While these methods have been successful at accurately modeling some systems, no approximation has accurately modelled every system. This is due to DFT not accounting for factors such as electron self-interaction and weak interactions, requiring corrections specialized for each system in order to get a higher degree of accuracy [1].

One goal in DFT is to try to get the accuracy of Kohn-Sham approach without the need for orbitals which can be expensive if lots of orbitals are needed, such as in most biochemistry calculations. This would combine the simplicity and quickness of TF theory without its lack of accuracy. [1] The thing that has to be fixed is in this case NOT the electron-electron interaction energy, but the kinetic energy, which in KS theory is an expression that uses the derivatives of the orbitals. However it is not yet understood how to express the kinetic energy effectively without orbitals [1].

Calculations to test these approximations and corrections can be quite costly in terms of computation time. One way to reduce the computation time is to perform these calculations in one dimension instead of the usual three. While sacrificing some accuracy, the lowered computational time allows for the quick testing of new theories that can be run on most computers. There are also a variety of potentials that are exactly solvable that can be used to test DFT models. We have written a code that can be used for this purpose and used the code to test common density approximations on one-dimensional equivalents for single-atom and diatomic-molecular systems.

Chapter 2

Theory

All calculations of the electronic structure of the atom require the many electron Schrödinger equation: [6]

$$H\Psi(x_1, x_2, ...x_N) = E\Psi(x_1, x_2, ...x_N). \tag{2.1}$$

The limits of x are from $-L$ to L. The Hamiltonian for the electronic structure of an atom in one dimension is: [6]

$$H(x_1, x_2, ..., x_N) = \sum_{i=1}^{N} V(x_i) + \sum_{i=1}^{N} \frac{-\hbar^2}{2m} \frac{d^2}{dx_i^2} + \frac{1}{2} \sum_{i \neq j} \sum_{i=1}^{j} V_{ee}(x_{ij}). \tag{2.2}$$

The total energy of the many-electron system is: [6]

$$E = \langle H \rangle = T + U_{ext} + U_{ee}. \tag{2.3}$$

Here each term is the expectation of each term in the Hamiltonian: [6]

$$U_{ext} = \int \Psi^*(x_1, x_2, ...x_N) \sum_{i=1}^{N} V(x_i) \Psi(x_1, x_2, ...x_N) dx_1 dx_2 \cdots dx_N, \tag{2.4}$$

and

$$T = \int, \Psi^*(x_1, x_2, ...x_N) \sum_{i=1}^{N} -\frac{\hbar^2}{2m} \frac{d^2\Psi(x_1, x_2, ...x_N)}{dx_i^2} dx_1 dx_2 \cdots dx_N \tag{2.5}$$

and

$$U_{ee} = \int \Psi^*(x_1, x_2, ...x_N) \frac{1}{2} \sum_{i=1, i \neq j}^{N} \sum_{j=1}^{N} V_{ee}(x_{i,j}) \Psi(x_1, x_2, ...x_N) dx_1 dx_2 \cdots dx_N. \tag{2.6}$$

The first two terms can be simplified through separation of variables with little issue, but the third term is more difficult since it depends on a function that links multiple variables. A practical application requires this to be simplified.

Conventional DFT, also called Kohn-Sham DFT, describes energy in terms of single particle orbitals [2]. Density is defined with the equation: [6]

$$n(x) = \sum_{i=1}^{N_{max}} |\phi_i(x)|^2. \tag{2.7}$$

The energy is defined with the equation: [6]

$$\langle H \rangle = E[n] = T + U_{ext} + U_{ee}. \tag{2.8}$$

Here T as defined above is approximated by [6]

$$T = T_{KS} + corrections \tag{2.9}$$

where

$$T_{KS} = \sum_i \int \psi_i^*(x) \left(-\frac{\hbar^2}{2m} \right) \frac{d^2}{dx^2} \psi_i(x) dx = \int \tau_{KS} dx. \tag{2.10}$$

Since we are using Hartree atomic units, $\hbar = m = 1$, so the equation becomes:

$$T_{KS} = -\frac{1}{2} \sum_i \int \psi_i^*(x) \frac{d^2}{dx^2} \psi_i(x) dx = \int \tau_{KS} dx. \tag{2.11}$$

Using integration by parts on the integral above, we get:

$$\int \psi_i^*(x) \frac{d^2}{dx^2} \psi_i(x) = \psi_i \frac{d\psi_i(x)}{dx} |_{-L}^{L} - \int \frac{d\psi_i(x)}{dx} \frac{d\psi_i(x)}{dx} dx. \tag{2.12}$$

Now in the case of the ψ's that we are using, it so happens that:

$$\frac{1}{2} \int \frac{d^2 |f(x)|^2}{dx^2} dx = f(x) \frac{df(x)}{dx}. \tag{2.13}$$

(Note: To demonstrate this, simply plug the basis function from Equation 3.4 into ψ in Equation 2.13.)

This means that Equation 2.12 can be rewritten as:

$$\int \psi_i^*(x) \frac{d^2}{dx^2} \psi_i(x) = \frac{1}{2} \int \frac{d^2 |\psi_i|^2}{dx^2} dx - \int \frac{d\psi_i}{dx} \frac{d\psi_i}{dx} dx. \tag{2.14}$$

If we plug the terms from equation 2.12 into equation 2.11, we get:

$$\tau(x) = -\frac{1}{2}\sum_i \psi_i(x)\frac{d^2}{dx^2}\psi_i(x) = \frac{1}{2}\left(\frac{1}{2}\sum_i \frac{d^2|\psi_i|^2}{dx^2}dx - \sum_i \frac{d\psi_i}{dx}\frac{d\psi_i}{dx}dx\right). \tag{2.15}$$

The main issue with this term is that the kinetic energy can become negative, so if we define a positive-definite kinetic energy density that is related to the kinetic energy density, but always positive. This is positive-definitie kinetic energy density is defined as:

$$\tau_{posdef} = \tau_{conventional} + \frac{1}{4}\sum_i \frac{d^2|\psi_i|^2}{dx}. \tag{2.16}$$

The result is:

$$\tau_{posdef} = \frac{1}{2}\sum_i \left|\frac{d\psi_i}{dx}\right|^2. \tag{2.17}$$

This equation is the equation that we used to calculate the KS kinetic energy density. U_{ext} and U_{ee} are found throught the equations:

$$U_{ext} = \int n(x)V(x)dx, \tag{2.18}$$

$$U_{ee} = \int\int n(x)V_{ee}(x-x')n(x')dxdx' + corrections. \tag{2.19}$$

Only T requires orbitals, as the rest just use the particle density. We set V_{ee} to 0, as we do not require it to study the issue of how to calculate the kinetic energy.

The advantage to conventional density functional theory is that a many electron problem is replaced by many single electron problems. The disadvantage to conventional density functional theory is that if the problem has too many orbitals, then the calculations for the electronic structure of the atom may still be too time consuming. Replacing $\tau(x)$ with a pure density expression would improve the speed of the calcutions greatly [6].

The kinetic energy density approximations that we used were the Kohn-Sham (KS), the Von Weizsäcker, the Thomas-Fermi, and the Gradient. The Kohn-Sham is accurate but still time consuming as the Kohn Sham still requires the calculation of many orbitals and is found through the equation: [6]

$$\tau_{KS} = \frac{1}{2}\sum_i \left|\frac{d\psi_i}{dx}\right|^2. \tag{2.20}$$

Strictly speaking the Kohn-Sham kinetic energy is the kinetic energy of a model system of noninteracting electrons used to model that of a system of interacting electrons. For our study we just ignored electron interactions. So, the KS τ is in our case the exact τ. The Von Weizs*ä*cker evaluates the system as if the electrons are bosons, so the Von Weizs*ä*cker is accurate only if there is one energy level. The Von Weizs*ä*cker is calculated through the equation: [6]

$$\tau_{VW} = \frac{1}{8}\frac{|\nabla n|^2}{n}. \tag{2.21}$$

The Thomas-Fermi evaluates the system as if there were an infinite number of electrons, so the Thomas-Fermi should become more accurate when there are more electrons in the system. The Thomas-Fermi is evaluated through the equation: [6]

$$\tau_{TF} = \frac{\pi^2 n^3}{24}. \tag{2.22}$$

The Local Gradient Expansion Kinetic Energy Density is a correction of the Thomas-Fermi that should be more accurate. The Local Gradient Expansion is calculated through the equation: [5]

$$\tau_G = \tau_{TF} - \frac{1}{3}\tau_{VW} + \frac{1}{12}\frac{d^2 n}{dx^2}. \tag{2.23}$$

To simulate a one-dimensional atom, we use a Poschl-Teller well potential. Poschl-Teller wells have many different interesting properties and uses, including the modeling of materials. [7, 8, 9, 10] Poschl-Teller well potentials are calculated through the equation: [11, 12]

$$V(x) = -\frac{\hbar^2}{2m}\alpha^2\frac{\lambda(\lambda+1)}{cosh^2\alpha x}. \tag{2.24}$$

The eigenenergies of a Poschl-Teller well are found through the equation: [11, 12]

$$E_k = -\frac{\hbar^2\alpha^2}{2m}(\lambda - k)^2. \tag{2.25}$$

Both α and λ are constants, with α determining the well width and λ determning the well depth. For this experiment, all of our runs use an α of 1.0 and a variety of different λs. The k's that result in a negative eigenenergy are the k's that have a bound state in the well. This means that we can alter λ to change the number of bound electron states. Poschl-Teller Wells

go to 0 at positive and negative infinity and are infinitely differentiable. The Poschl-Teller Well is closer to approximating a Coulomb potential than a Square Well model would be, and the Poschl-Teller Well's differentiability creates cleaner results.

When we talk about Poschl-Teller Double Wells, these consist of two Poschl-Teller Wells superimposed on each other with some sort of distance between the centers of the wells. We calculate this, with d being the distance between the center of the wells, using the equation:

$$V_{double}(x) = V(x - \frac{d}{2}) + V(x + \frac{d}{2}). \tag{2.26}$$

2.1 ELF

A useful value to identify electronic structure and molecular bond type is the Electron Localization Function (ELF) [13]. The ELF is calculated through the equations: [13]

$$ELF = \frac{1}{1 + \alpha^2}, \tag{2.27}$$

$$\alpha = \frac{\tau_{KS} - \tau_{VW}}{\tau_{TF}}. \tag{2.28}$$

(Note: This α is a different α than the α in the equation for the Poschl-Teller Well.) The ELF ranges from 0.0 to 1.0 in value. An ELF close to 1.0 indicates covalent properties. An ELF close to 0.5 indicates metallic properties. An ELF close to 0.0 indicates ionic properties.

Chapter 3

Methods

For all of our calculations, we use Hartree atomic units, which are useful because Hartree atomic units result in $\hbar = e = m = \frac{4\pi}{\epsilon_0} = 1$. This means that all of those variables can be ignored in the calculations. We used an algorithm from a book [12] that expresses orbitals as a linear combination of plane waves on a finite-width cell. This code, written in Python, constructs a matrix by multiplying the potential by two basis functions, and then adding kinetic energies along the diagonal. We constructed each matrix element, with the matrix element represented by $H_{i,j}$, with the equation:

$$H_{i,j} = E_j \delta_{i,j} + \int_{-L}^{L} \phi_i^* V(x) \phi_j dx. \tag{3.1}$$

This equation is derived from the following equations:

$$H = -\frac{\hbar^2}{2m}\frac{d^2}{dx^2} + V(x), \tag{3.2}$$

$$H_{i,j} = \int \phi_i(x) H \phi_j(x) dx = \int \phi_i(x)(-\frac{\hbar^2}{2m})(\frac{d^2}{dx^2})\phi_j(x)dx + \int \phi_i(x) V(x) \phi_j(x) dx. \tag{3.3}$$

We compared our results to results from the book [12] to make sure that we were accurate. We use the linalg library in the numpy Python libraries to get the eigenvalues and eigenvector coefficients of this matrix.

The plane wave basis functions that we used were:

$$\phi_i(k) = sin\left(\frac{\pi(k-L)}{2L}\right). \tag{3.4}$$

The plane wave basis functions meet the boundary conditions that the function is 0 at $x = -L$ and $x = L$.

The orbitals were obtained through the equation:

$$\psi_i(x) = \sum_{n=1}^{N_{max}} C_n^i \phi_n(x) \tag{3.5}$$

with C_n^i as the eigenvector coefficient calculated from doing the eigenvalue problem of the matrix.

The number of basis functions used was calculated through the equation:

$$N_{max} = \frac{1}{\pi}\sqrt{2E_{cut}}. \tag{3.6}$$

We test the convergence of the variables E_{cut} and L. We could then obtain a result for the particle density of the system through the equation: [6]

$$n(x) = \sum_i f_i |\sum_n C_n^i \phi_n(x)|^2 \tag{3.7}$$

where f_i is the number of electrons in orbital i.

We get the Kohn-Sham kinetic energy density through the equation: [6]

$$\tau(x) = \sum_i f_i |\sum_n C_n^i \phi_n'(x)|^2. \tag{3.8}$$

To integrate any function, we used Composite Simpson Integration, which uses the equation for an array of data taken from a function $f(x)$:

$$\int f(x)dx = \frac{dx}{3}(f_{First} + 4\sum f_{Odds} + 2\sum f_{Evens} + f_{Last}). \tag{3.9}$$

To find derivatives, we used the equation: [14]

$$\frac{df(x_i)}{dx} = \frac{1}{dx}\left[\frac{2}{3}(f(x_{i+1}) - f(x_{i-1})) - \frac{1}{12}((f(x_{i+2}) - f(x_{i-2}))\right]. \tag{3.10}$$

We used this because the results were smoother than a normal centered derivative.

Chapter 4

Results

4.1 Calibration and testing

We started by testing square wells, but the nondifferentiability of the potential resulted in data that took too long to converge. We then tested the convergence of Poschl-Teller wells with regard to E_{cut} and L. The results are in Figure 4.1.

While an E_{cut} value of 50 was sufficient for these systems, to properly graph some of the more difficult to converge plots, we found that we needed E_{cut}'s ranging from 300 to even 1200. The plots of the resulting wavefunctions are in Figure 4.2.

Both energy states converge reasonably for E_{cut}. The ground state shows no correlation to L, and all answers agree within 5 significant figures. The first excited state improves as L increases but never converges to the expected value of 0. The reason can be seen in the wavefunction graph, as the resulting wavefunction should look like a flat line, but it would require an impractically large L to create an acceptable wavefunction. Because of this, we used half-integer values for λ, which resulted in only bound states.

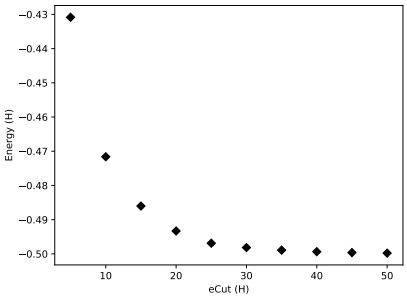

(a) Ground State E_{cut} Convergence

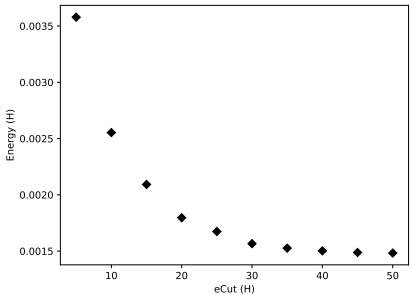

(b) First Excited State E_{cut} Convergence

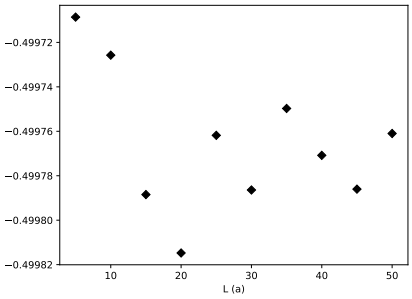

(c) Ground State L Convergence

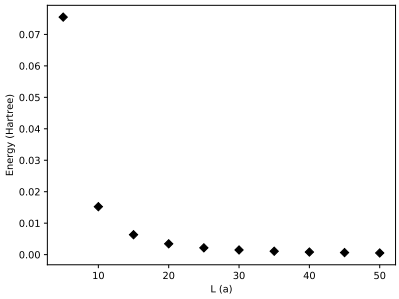

(d) First Excited State L Convergence

Figure 4.1: Poschl-Teller Well Convergence Tests for $\lambda = 1.0$

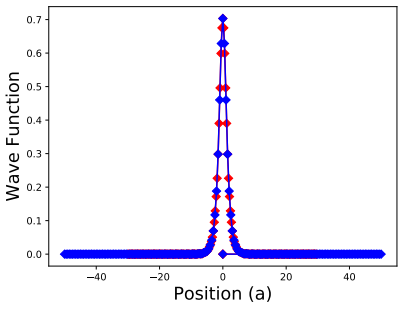

(a) Ground State

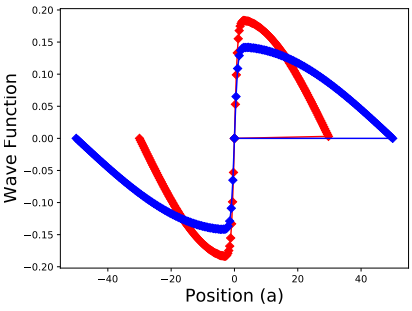

(b) First Excited State

Figure 4.2: Poschl-Teller Well Wavefunctions. Red: $L = 30$ Blue: $L = 50$

4.2 Kinetic Energy Plots for Single Wells

We plotted the kinetic energies of single Poschl-Teller Wells for various half-integer λ's. For every plot shown after this point, we filled every available bound state for each system with an electron. The resulting plots are in Figure 4.3. In Figure 4.3a, as predicted, the TF is a poor approximation of the kinetic energy density and the VW is an exact estimate of the kinetic energy density. Unexpectedly, the gradient approximation is also an exact estimate for the kinetic energy densities. As the graphs with more electrons show, as electrons are added the TF becomes more and more of an accurate estimate of the kinetic energy density and the VW quickly becomes completely inaccurate. The gradient unexpectedly continues to be an apparent exact estimate.

4.3 Particle Density Plots for Single Wells

We plotted the particle densities of single Poschl-Teller Wells for various half-integer λ's. The resulting plots are in Figure 4.4. We cannot see any electronic shell structure in these graphs which is different than what is usually found in systems like this. [15] The curve shapes appear to be identical between the plots of the various different systems of various different λ's.

4.4 Kinetic Energy Density Approximation Plots for Double Wells

We plotted the kinetic energy density approximations of double Poschl-Teller Wells for various half-integer λs and distances between the wells. For $\lambda = 0.5$ we had 2 electrons, for $\lambda = 1.5$ we had 6 electrons, and for $\lambda = 2.5$ we had 10 electrons. The results are in Figure 4.5, Figure 4.6, and Figure 4.7. In Figure 4.5, the graphs show that the VW continues to be an exact estimate when we have only one energy level of electrons and the TF continues

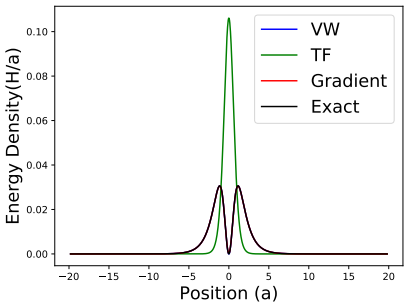

(a) 0.5 λ, 2 electrons

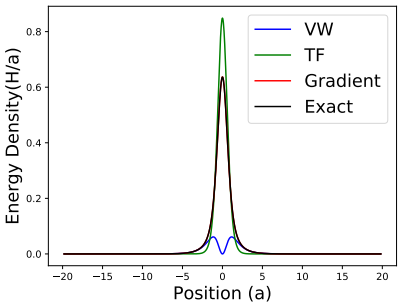

(b) 1.5 λ, 4 electrons

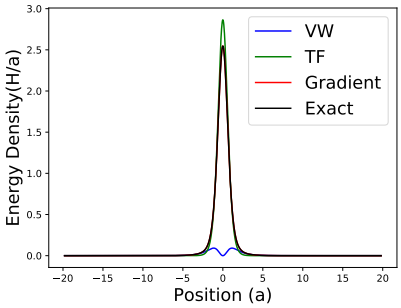

(c) 2.5 λ, 6 electrons

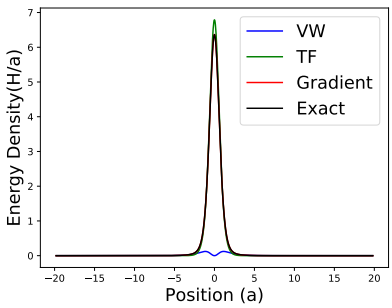

(d) 3.5 λ, 8 electrons

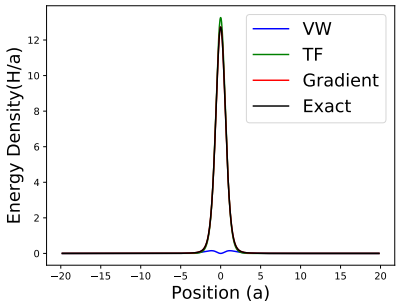

(e) 4.5 λ, 10 electrons

Figure 4.3: Single Poschl-Teller Well Kinetic Energy Density Approximations

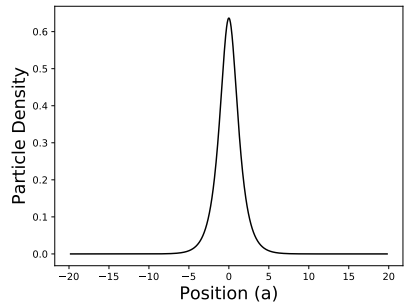

(a) 0.5 λ, 2 electrons

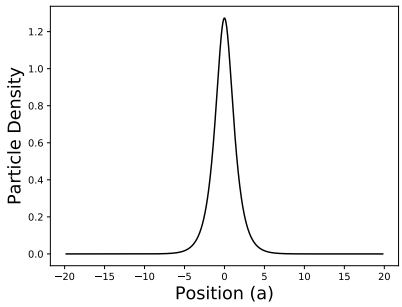

(b) 1.5 λ, 4 electrons

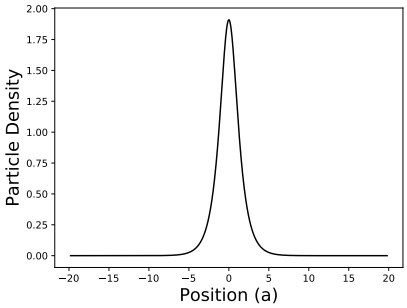

(c) 2.5 λ, 6 electrons

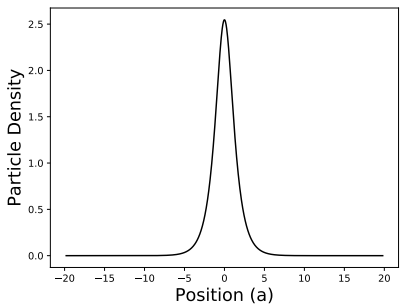

(d) 3.5 λ, 8 electrons

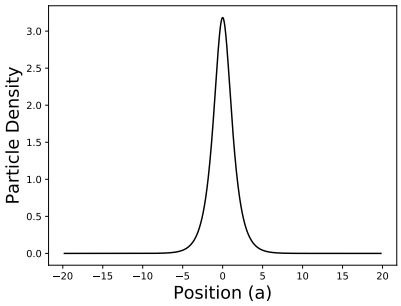

(e) 4.5 λ, 10 electrons

Figure 4.4: Single Poschl-Teller Well Particle Densities

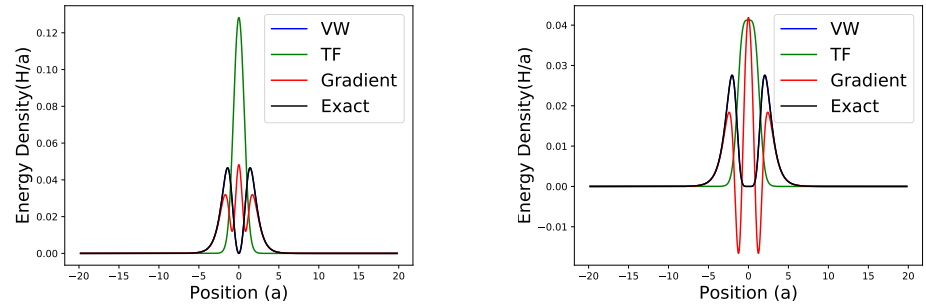

(a) 1.5 distance

(b) 2.5 distance

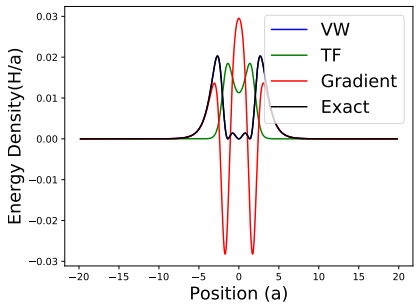

(c) 3.5 distance

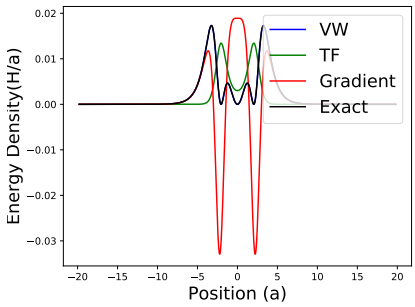

(d) 4.5 distance

Figure 4.5: Double Poschl-Teller Well Kinetic Energy Density Approximations for $\lambda = 0.5$

to be a poor estimate when there is only one energy level of electrons. For this double well system, the gradient fails completely, Not only is the gradient not close at all to the KS, it becomes negative at several points, which according to the theory, should not happen. This appears to be the only case where the gradient approximation is this poor. In Figure 4.6a, the graph shows that the VW is a poor estimate of the kinetic energy density, while both the TF and the gradient kinetic energy approximations are both fairly accurate. As the wells are moved farther apart in the subsequent graphs in Figure 4.6, the TF becomes increasingly inaccurate, the gradient approximation is still accurate but not as accurate as the gradient approximation is in the single well plots, as seen in Figure 4.3, and the VW continues to be a poor estimation. The graphs in Figure 4.7 behave largely the same as the graphs in Figure 4.6.

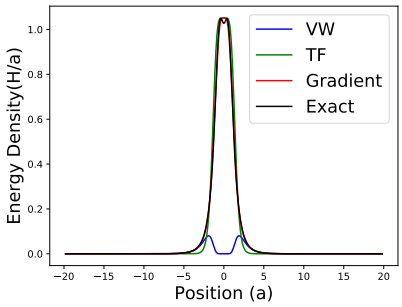

(a) 1.5 distance

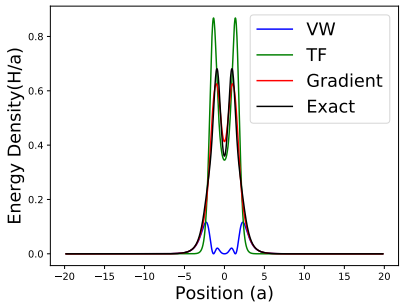

(b) 2.5 distance

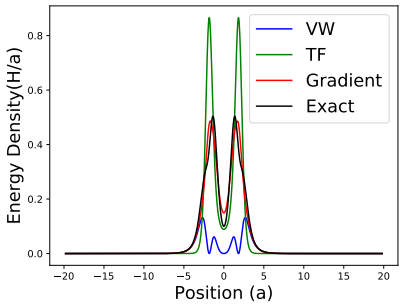

(c) 1.5 distance

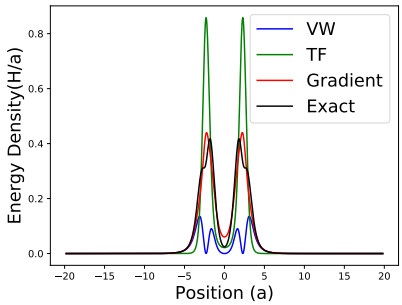

(d) 4.5 distance

Figure 4.6: Double Poschl-Teller Well Kinetic Energy Density Approximations for $\lambda = 1.5$

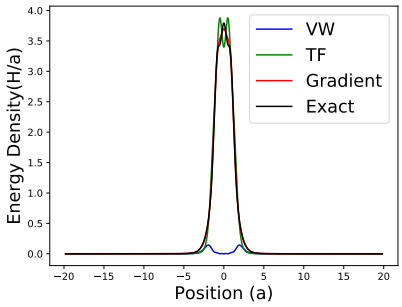

(a) 1.5 distance

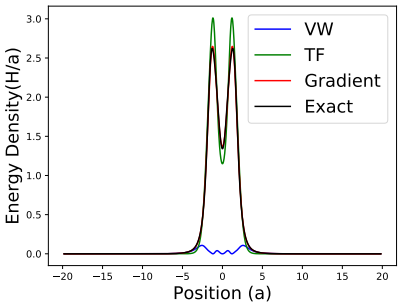

(b) 2.5 distance

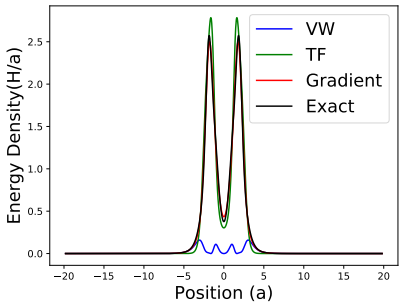

(c) 3.5 distance

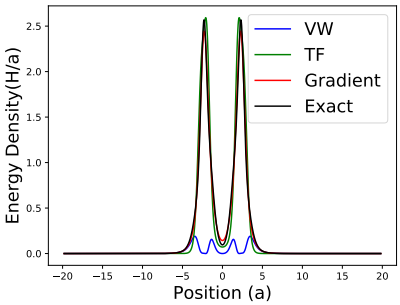

(d) 4.5 distance

Figure 4.7: Double Poschl-Teller Well Kinetic Energy Density Approximations for $\lambda = 2.5$

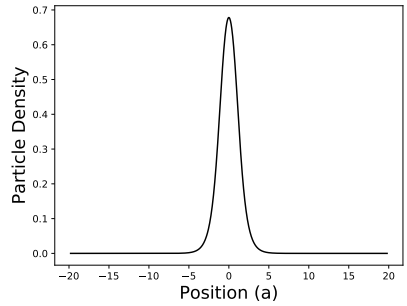

(a) 1.5 distance

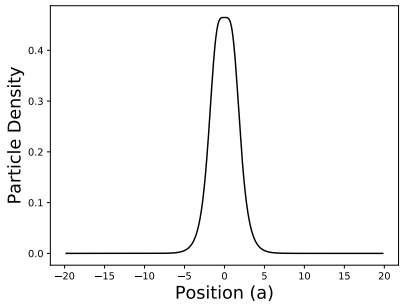

(b) 2.5 distance

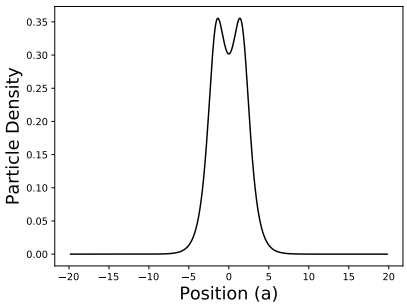

(c) 3.5 distance

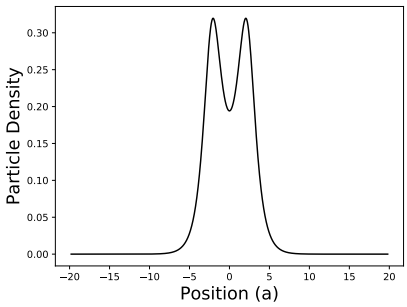

(d) 4.5 distance

Figure 4.8: Double Poschl-Teller Well Particle Densities for $\lambda = 0.5$

4.5 Particle Density Approximation Plots for Double Wells

We plotted the particle densities of double Poschl-Teller Wells for various half-integer λs and distances between the wells. The results are in Figure 4.8, Figure 4.9, and Figure 4.10. We can see from these graphs that the wells are never moved far enough apart to break the bond between the two atoms.

4.6 Further Analysis

We attempted to graph the total kinetic energy approximations for single wells on the y-axis, found by integrating the kinetic energy densities, with the λ's on the x-axis in order to see

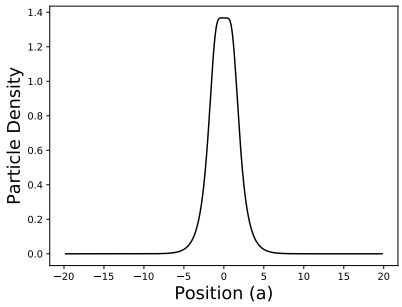

(a) 1.5 distance

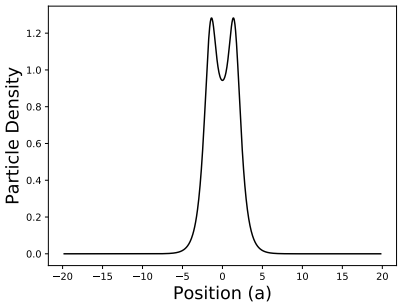

(b) 2.5 distance

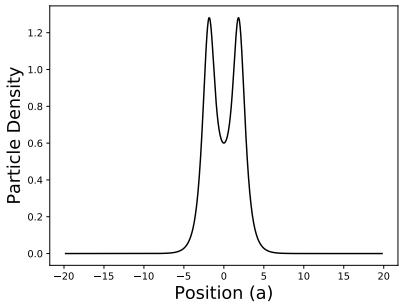

(c) 3.5 distance

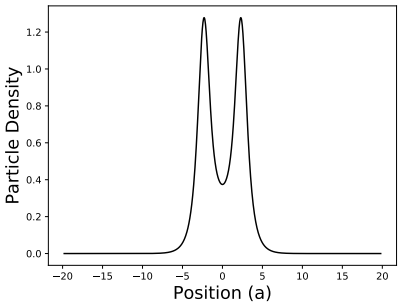

(d) 4.5 distance

Figure 4.9: Double Poschl-Teller Well Particle Densities for $\lambda = 1.5$

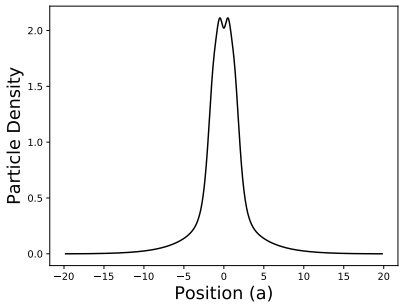

(a) 1.5 distance

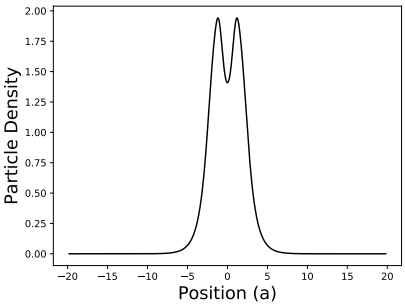

(b) 2.5 distance

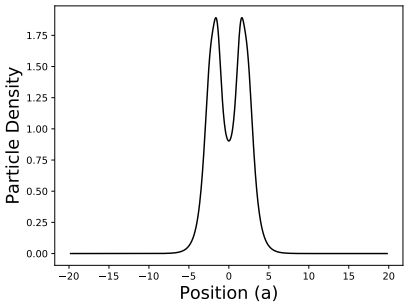

(c) 3.5 distance

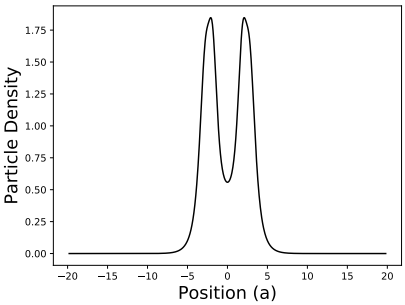

(d) 4.5 distance

Figure 4.10: Double Poschl-Teller Well Particle Densities for $\lambda = 2.5$

the differences between the approximations. This did not work very well because, as can be seen in Figure 4.11, all of the kinetic energy approximations were too close together to accurately compare them. To better see how the kinetic energy approximations compared as

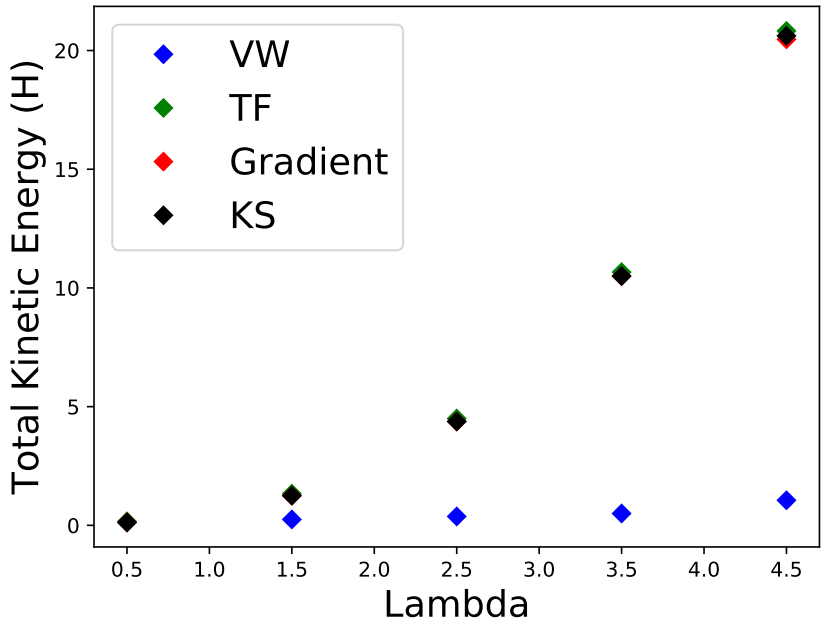

Figure 4.11: A Plot of the Kinetic Energy Approximations Versus λ

we added energy levels, we scaled the kinetic energy approximations by dividing the kinetic energy approximations by the number of filled energy levels cubed. The resulting plot is in Figure 4.12.

We graphed the ELF for the various single well system for a variety of λ's. The results are in Figure 4.13. Unusually, the ELF appears to be mostly flat, and there is no electronic structure visible in the ELF.

We graphed the particle densities for various λ's divided by the number of electrons, including a theoretical model that was calculated through a simple equation. [8] The results are in Figure 4.14. It can be seen that, rather unusually, the scaled particle densities are effectively identical in each case.

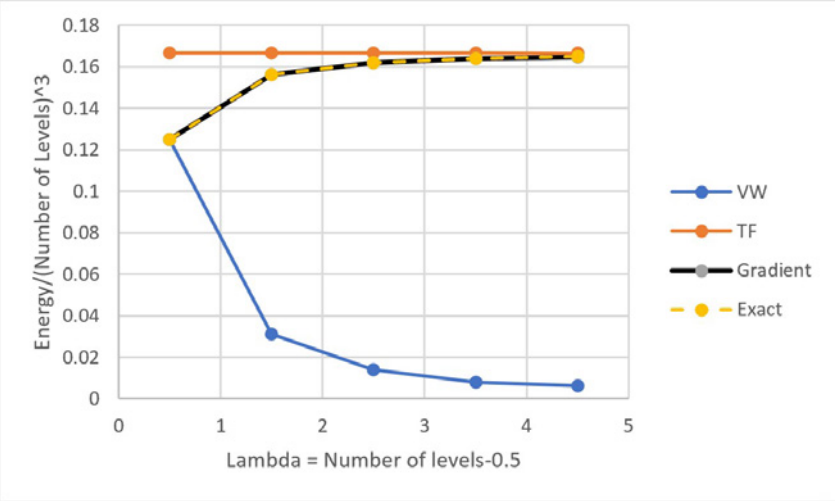

Figure 4.12: A Plot of the Kinetic Energy Approximations Divided by the Number of Energy Levels Cubed

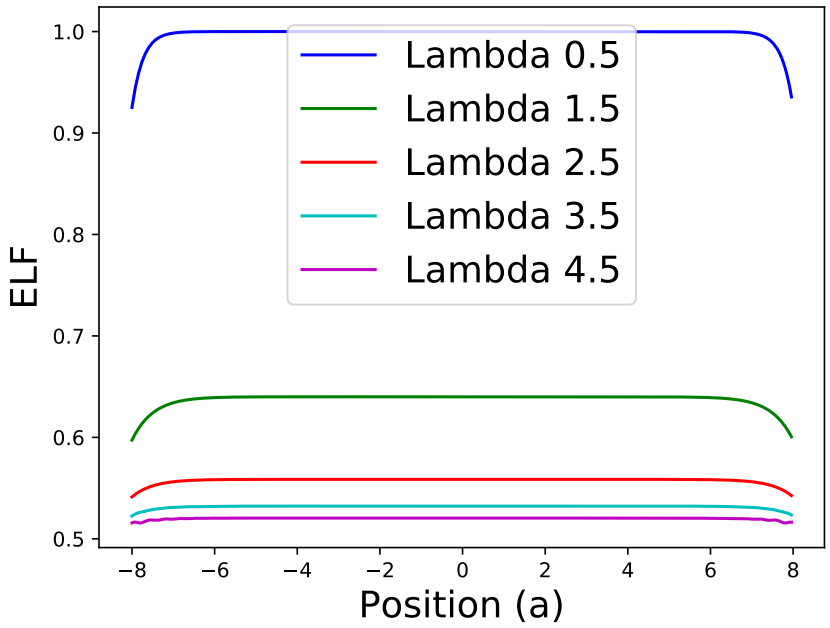

Figure 4.13: A Plot of the ELF for Single Wells for a Variety of λ's

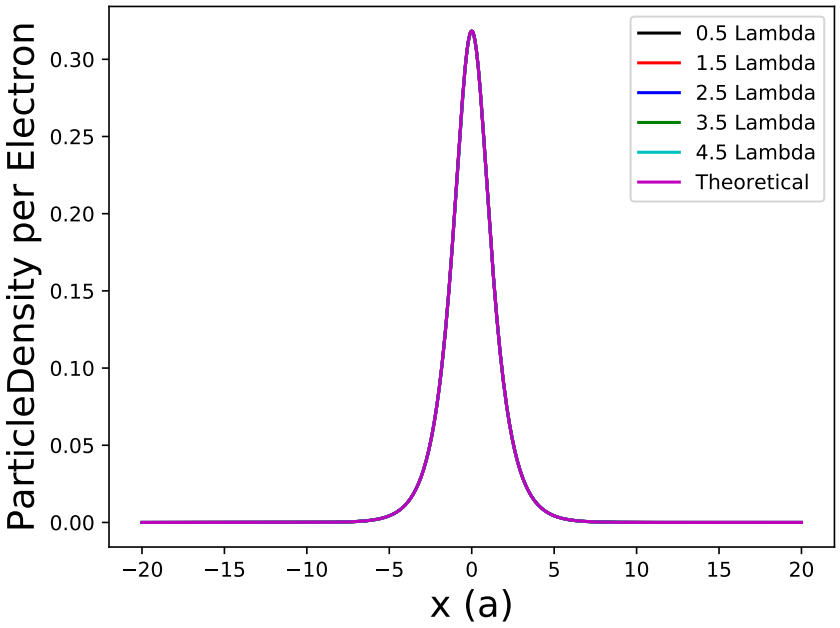

Figure 4.14: A Plot of the Particle Densities Divided by the Number of Electrons for Single Wells for a Variety of λ's

Chapter 5

Conclusion

We used python code to model atoms in one dimension using Poschl Teller Wells. We then filled the wells with electrons and then used matrices to calculate the orbitals. From the orbitals we calculated the particle density and the Kohn-Sham kinetic energy density. We then used the particle density to calculate a variety of other kinetic energy density approximations. We then graphed the kinetic energies and particle densities as well as the ELF. Our model performed as we expected in some circumstances. The VW approximation collapses whenever a system has electrons in any energy level beyond the ground state, the TF approximation improves when more electrons are added to the system, and the Gradient Density approximation is usually the most accurate, especially in one well systems. There were some unexpected results. For the ELF, the system for one-half λ is covalent, and the system becomes more metallic as electrons are added, but there is no sign of any electronic structure, which is unexpected. The TF approximation divided by the number of energy levels cubed is constant for all values of λ, which is an unusual property. There is also no sign of electronic structure in the kinetic energy graphs. Our scaled particle densities were identical no matter how many electrons we added, which is an unusual result in mathematical physics. For further research, the code could to test other systems, types of potentials, and types of approximations. There could also be a mathematical analysis of why there appears to be no electronic structure in these systems or why the scaled particle density remains the

same no matter the properties of the system.

Appendix A

Description of code

These make up the engine of my code. I use these in scripts to do various tasks to obtain my results.

CompositeSimpsonIntegration Integrates an array of values

densityCalculator Calculates the KS kinetic energy density and the particle density

DerivativeCalculator Calculates rge derivative and double derivative of an array

DFT Calculates the VW, TF, and localized gradient kinetic energy densities and then writes a kinetic energy density file

ELF Calculator Calculates the ELF

FileReader Reads particle density and kinetic energy density files

FileWriter Writes particle density and kinetic energy density files

GradientDensityCalculator Calculates the localized gradient kinetic energy density

MatrixBuilder Builds the matrix that we use to get the ψ values

plotter Contains functions that make plotting easier

potentials Contains functions that calculate the potential at a point in space for several different potential types

SiCalculator Calculates the ψ values for a system

TFCalculator Calculates the TF kinetic energy density

vwCalculator Calculates the VW kinetic energy density

wavefunctions Contains the wavefunction and the derivative of the wavefunction

Below are some examples of scripts that I used to create these plots.

WriteParticleDensityFilesForAllLambda This script writes files containing the positions, particle densities, and KS kinetic energy densities half-integer λ's from 0.5 to 4.5 for single Poschl-Teller wells.

WriteKineticEnergyDensityFilesForAllLambda This script takes particle density files for single Poschl-Teller wells with half-integer λ's from 0.5 to 4.5 and uses it to write a file that contains the position, particle density, VW kinetic energy density, TF kinetic energy density, localized gradient kinetic energy density, and the KS kinetic energy density.

AllKEApproximationsForAllLambdaUsingFiles This script takes kinetic energy density files for single Poschl-Teller wells with half-integer λ's from 0.5 to 4.5 and uses it to make plots that contain all of the KE approximations used versus the position

Bibliography

[1] Aurora Pribram-Jones, David A. Gross, and Kieron Burke. *DFT: A Theory Full of Holes? The Annual Review of Physical Chemistry* **66**, 283 (2015).

[2] W. Kohn and L. J. Sham. *Self-Consistent Equations Including Exchange and Correlation Effects. Physical Review* **140**, 1133 (1965).

[3] L. H. Thomas. *The calculation of atomic fields. Math. Proc. Camb. Phil. Soc.* **23(05)**, 542 (1927).

[4] E. Fermi. *Eine statistische Methode zur Bestimmung einiger Eigenschaften des Atoms und ihre Anwendung auf die Theorie des periodischen Systems der Elemente (a statistical method for the determination of some atomic properties and the application of this method to the theory of the periodic system of elements). Zeitschrift für Physik A Hadrons and Nuclei* **48**, 73 (1928).

[5] L. Samaj and J. K. Percus. *Recursion representation of gradient expansion for free fermion ground state in one dimension. The Journal of Chemical Physics* **111(5)**, 1809 (1999).

[6] Richard Lesar. *Introduction to Computational Materials Science: Fundamentals to Applications.* Cambridge University Press (2013).

[7] R. R. Hartmann and M. E. Portnoi. *Two-Dimensional Dirac Particles in a Poschl-Teller Waveguide. Scientific Reports* **7** (2017).

[8] G. Hunter, P. Ecimovic, I. Schlifer, I. M. Walker, D. Beamish, S. Donev, M. Kowalski, S. Arslan, and S. Heck. *Fermion quasi-sphere harmonics. Journal of Physics A: Mathematical and General* **32**, 795 (1999).

[9] J. Radovanovic, V. Milanovic, Z. Ikonic, and D. Indjin. *Intersubband Absorption in Poschl-Teller-Like Semiconductor Quantum Wells. Physics Letters A* **269**, 179 (2000).

[10] B. Y. Tong. *Scattering states of the sech-squared potential. Solid State Communications* **104**, 679 (1997).

[11] G. Pöschl and E. Teller. *Bemerkungen zur quantenmechanik des anharmonischen oszillators. Zeitschrift für Physik* **83(3)**, 143 (Mar 1933).

[12] Paul Harrison. *Computational Methods in Physics, Chemistry, and Biology: An Introduction.* John Wiley and Sons, LTD (2001).

[13] A. D. Becke and K. E. Edgecombe. *A Simple Measure of Electron Localization in Atomic and Molecular Systems. The Journal of Chemical Physics* **92(9)**, 5397 (1990).

[14] Milton Abramowitz and Irene A. Stegan, editors. *Handbook of Mathematical Functions.* Dover Publishing, ninth edition (1972).

[15] Alfred M. Simas, Robin P. Sagar, Andrew C. T. Ku, and Vedene H. Smith Jr. *The radial charge distribution and the shell structure of atoms and ions. Canadian Journal of Chemistry* **66(8)**, 1923 (1988).